



Mesoporous Iron Trifluoride Microspheres as Cathode Materials for Li-ion Batteries



Zhen Long^{a,d}, Wenyuan Hu^a, Lihu Liu^b, Guohong Qiu^b, Wencan Qiao^b,
Xiangfeng Guan^c, Xiaoqing Qiu^{d,*}

^a State Key Laboratory Cultivation Base for Nonmetal Composites and Functional Materials, Southwest University of Science and Technology, Mianyang 621010, China

^b College of Resources and Environment, Huazhong Agricultural University, Wuhan 430070, China

^c Institute of advanced photovoltaics, College of electronics and information science, Fujian Jiangxia University, Fuzhou 350108, China

^d Research Institute of Photocatalysis, State Key Laboratory of Photocatalysis on Energy and Environment, College of Chemistry, Fuzhou University, Fuzhou 350002, China

ARTICLE INFO

Article history:

Received 27 July 2014

Received in revised form 14 October 2014

Accepted 5 November 2014

Available online 7 November 2014

Keywords:

Iron trifluoride

Cathode materials

Lithium ion batteries

Electrochemical properties

ABSTRACT

Mesoporous $\text{FeF}_3(\text{H}_2\text{O})_{0.33}$ microspheres, hexagonal columns, and $\beta\text{-FeF}_3 \cdot 3\text{H}_2\text{O}$ square microrods have been prepared via facile solution methods using polyethylene glycol, oleic acid, and dodecyl trimethyl ammonium chloride as a surfactant, respectively. The as-prepared mesoporous $\text{FeF}_3(\text{H}_2\text{O})_{0.33}$ microspheres exhibits an enhanced lithium storage capacity and excellent cycling stability ($159.2 \text{ mA h g}^{-1}$ at 142 mA g^{-1} after 100 cycles). Even at a high current density of 474 mA g^{-1} , mesoporous $\text{FeF}_3(\text{H}_2\text{O})_{0.33}$ microspheres still deliver a discharge capacity as large as 95.9 mA h g^{-1} after 100 cycles. This remarkable electrochemical performance can be attributed to the high specific surface area and mesoporous microspherical structure, which effectively increase the contact area between the active materials and the electrolyte, reducing the Li-ion diffusion pathway and buffering the volume change during cycling.

© 2014 Elsevier Ltd. All rights reserved.

1. Introduction

The global imperative for rechargeable lithium ion batteries needs to develop novel cathode materials comprised of inexpensive, non-toxic and earth-abundant elements [1–7]. Metal fluorides have attracted considerable interest as next-generation high capacity electrode materials, since they can offer the full utilization of redox and show multi-electron capacity compared to the traditional cathode materials, such as LiCoO_2 , LiMn_2O_4 , and so on [8]. Among the various metal fluorides, iron trifluoride (FeF_3) is considered as an important and prominent cathode material owing to its high electromotive force, low toxicity and natural abundance [9,10]. The strong ionic character of Fe-F bond in FeF_3 provides high operation voltage during Li^+ ion insertion and deinsertion [11]. Moreover, FeF_3 has higher capacity and cheaper than the current commercial LiCoO_2 cathode [12]. However, the practical utilization of FeF_3 has been retarded by its low conductivity, sluggish kinetics, and poor cycle stability. Accordingly, many elaboration works have been done to enhance the above characters

of FeF_3 , mainly focusing on the improvement of the electronic conductivity by conductive coating and introducing conductive additives on the active material [11–16]. For instance, FeF_3/C nanocomposites were prepared by Amatucci et al. using a high-energy mechanical milling method, which displayed high capacity but low cycle stability at 7.58 mA g^{-1} [13]. Kang's group reported the fabrication of FeF_3 nano-flowers on the carbon nano-tubes, which delivered discharge capacities of 210 and 150 mA h g^{-1} between 2.0 and 4.5 V at current densities of 20 and 500 mA g^{-1} , respectively [17]. Unfortunately, conductive carbon surface coating results in the negative effects on the tap density in the composite electrode [18]. Effective control of the growth and morphology is well demonstrated to be an alternative approach to improve the battery performance of the electrode materials [19,20]. For example, Tarascon and his coworkers employed the pulsed laser deposition method to grow the FeF_3 thin film with good cycling life [21,22]. Li et al. synthesized nanostructured $\text{FeF}_3 \cdot 0.33 \text{ H}_2\text{O}$ with a sponge-like morphology by using a low-temperature ionic liquid as a solvent and fluorine source, which deliver initial discharge capacities of 160 and 126 mA h g^{-1} between 1.6 and 4.5 V at current densities of 14 and 71 mA g^{-1} , respectively [9]. Recently Zhang et al. fabricated macroporous FeF_3 hybrids with superior rate performance by applying the colloidal crystal template technique [23].

* Corresponding author. Tel.: +86 591 83969021; fax.: +86 591 83969021.

E-mail address: qiuxq@fzu.edu.cn (X. Qiu).

Indeed, mesoporous structure of the electrode materials is well known to be beneficial for the Li storage and effective contact between the electrolyte and electrode, thereby offering fast and flexible transport pathways for the electrolyte infiltration and free space to tolerate the volume change during cycling [23,24]. On the other hand, the spherical materials are considered as the optimal candidates for the lithium ion batteries, because they have high pile-density, high capacity density and excellent particle mobility to form a compact electrode layer [25]. Despite the recent significant progress, the performance of the FeF_3 cathode is still far from satisfactory and there is little study on the synthesis of mesoporous FeF_3 microspheres and their electrochemical performance.

Herein, micro-spherical mesoporous $\text{FeF}_3 \cdot (\text{H}_2\text{O})_{0.33}$ sample is first prepared by a solution method using polyethylene glycol 20,000 (PEG-20000) as a surfactant. As a cathode material, the mesoporous $\text{FeF}_3 \cdot (\text{H}_2\text{O})_{0.33}$ microspheres show an excellent cycling life with a discharge capacity of $159.2 \text{ mA h g}^{-1}$ at 142 mA g^{-1} after 100 cycles in a voltage range of 2.0–4.5 V and a good rate capability with a discharge capacity up to 95.9 mA h g^{-1} at a high current density of 475 mA g^{-1} after 100 cycles. Additionally, to study the effect of morphology and content of crystal water on physical and chemical properties of FeF_3 cathode, the $\text{FeF}_3(\text{H}_2\text{O})_{0.33}$ hexagonal columns and $\beta\text{-FeF}_3 \cdot 3\text{H}_2\text{O}$ square microrods are also synthesized in this work via facial solution methods.

2. Experimental section

2.1. Synthesis of mesoporous $\text{FeF}_3 \cdot (\text{H}_2\text{O})_{0.33}$ microspheres

Typically, 40 mL of iron nitrate nonahydrate ($\text{Fe}(\text{NO}_3)_3 \cdot 9\text{H}_2\text{O}$) ethanol solution with a concentration of 0.5 mol/L was added in 150 mL of 5.5 mmol/L PEG-20000 ethanol solution to give a clear solution, named solution *a*. Meanwhile, 20 mL of 3 mol/L ammonium fluoride solution was also added in another 150 mL of 5.5 mol/L PEG-20000 ethanol solution to form a clear solution, solution *b*. Then, the solution *a* was added slowly into the solution *b* at room temperature. After stirring for about 2 h, the sample was collected by centrifuging and sufficient washing with ethanol and then dried at ambient conditions.

2.2. Synthesis of $\text{FeF}_3(\text{H}_2\text{O})_{0.33}$ hexagonal columns

The $\text{FeF}_3 \cdot (\text{H}_2\text{O})_{0.33}$ hexagonal columns were prepared in mixed solvent of water and ethanol through one-step hydrothermal method. Briefly, 8.0802 g (0.02 mol) of $\text{Fe}(\text{NO}_3)_3 \cdot 9\text{H}_2\text{O}$ was dissolved in an appropriate amount of ethanol. Then, 8 mL of oleic acid and a certain volume of deionized water were added in ethanol solution. The total volume of water and ethanol is 40 mL. After ultrasound for about 10 min, 3 mL of hydrofluoric acid (HF, 40 wt.%) was added in the above solution to form a suspension, which was transferred into a 60 mL Teflon-lined autoclave. The autoclave was kept at 120°C for 12 h. Finally, the samples were achieved by centrifuging and washing with ethanol.

2.3. Synthesis of $\beta\text{-FeF}_3 \cdot 3\text{H}_2\text{O}$ square microrods

Firstly, 25 g of dodecyl trimethyl ammonium chloride (DTAC) was added in 150 mL of acetone. After stirring for about 2 h, the acetone solution was divided into two parts. Then, 20 mL of 1 mol/L $\text{Fe}(\text{NO}_3)_3 \cdot 9\text{H}_2\text{O}$ solution was added in the one part of acetone solution, and 3 mL hydrofluoric acid (HF, 40 wt.%) was added in the other part. Stirring for about 2 h again, the above two solutions were mixed and stirred for 2 h. the sample was gained by centrifuging the aqueous layer and washing with ethanol.

2.4. Sample characterization

Fourier transform infrared (FTIR) spectra of the samples were measured on an Equinox55 IR spectrophotometer with a resolution of 4 cm^{-1} by the KBr pellet technique. Crystalline phase of the synthesized materials were identified by X-ray diffraction (XRD) on a Bruker D8 Advance X-ray diffractometer using $\text{Cu K}\alpha$ ($\lambda = 1.5418 \text{ \AA}$) radiation. The thermal behaviors and water contents of the as-obtained samples were examined with a Netzsch STA449C thermogravimetric (TG) analyzer at a heating rate of $15^\circ\text{C min}^{-1}$ from room temperature to 850°C in a N_2 atmosphere at a flux of 30 mL min^{-1} and under ambient atmospheric pressure. Brunauer-Emmett-Teller (BET) specific surface areas were examined on a JEDL-6390/LV Automatic specific surface analyzer. The particle morphology and size of the samples were determined by field emission scanning electron microscopy (SEM) on a JEOL JSM-6390/LV instrument under an acceleration voltage of 5 kV. The cyclic voltammograms (CV) and electrochemical impedance spectroscopy (EIS) were measured using an electrochemical workstation (CHI660B).

2.5. Electrochemical test

Electrochemical performance of the samples was measured using the CR-2032-type coin cell. The cathode mixtures consisted of 40 wt.% synthesized powders sample dried at 100°C for 6 h, 40 wt.% acetylene black and 20 wt.% polytetrafluoroethylene binder on the aluminum mesh. The cells were assembled in an argon-filled glove box (H_2O and $\text{O}_2 < 5 \text{ ppm}$) using lithium foil as the anode, a polymer separator and 1 M LiPF_6 in EC:EMC:DMC (1:1:1 in volume) as the electrolyte. The cell was charged and discharged galvanostatically in a voltage range of 2.0–4.5 V at 25°C with different current densities of 142, 190, 237, and 474 mA g^{-1} .

3. Results and Discussion

Fig. 1 shows the XRD pattern of sample obtained at room temperature by using PEG-20000 as a surfactant. The standard data for bulk $\text{FeF}_3 \cdot (\text{H}_2\text{O})_{0.33}$ (JCPDS Card No. 76–1262) and $\beta\text{-FeF}_3 \cdot 3\text{H}_2\text{O}$ (No. 32–0464) are also presented for comparison. It is shown that the diffraction peaks are relatively strong and the peak positions matched well the standard data for bulk $\text{FeF}_3 \cdot (\text{H}_2\text{O})_{0.33}$. No impurity peaks associated with $\text{Fe}_{1.9}\text{F}_{4.75} \cdot (\text{H}_2\text{O})_{0.95}$ [9], $\beta\text{-FeF}_3 \cdot 3\text{H}_2\text{O}$, iron oxides and iron oxyhydroxides [26] were

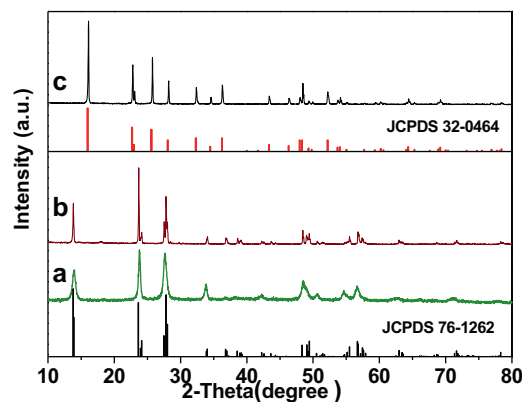


Fig. 1. XRD patterns of the samples obtained under different conditions. (a) at room temperature by using PEG-2000 as a surfactant, (b) in a mixed solvent of water and ethanol under hydrothermal condition at 120°C for 12 h, (c) by using DTAC as a surfactant. Vertical bars below the patterns represent the standard diffraction data from JCPDS file for bulk $\text{FeF}_3(\text{H}_2\text{O})_{0.33}$ (No. 76–1262) and $\beta\text{-FeF}_3 \cdot 3\text{H}_2\text{O}$ (No. 32–0464).

Download English Version:

<https://daneshyari.com/en/article/184847>

Download Persian Version:

<https://daneshyari.com/article/184847>

[Daneshyari.com](https://daneshyari.com)